Digest Journal of Nanomaterials and Biostructures Vol. 8, No. 1, January - March 2013, p. 423 - 431

SYNTHESIS AND CHARACTERIZATION OF Mg-Al ALLOYS FOR HYDROGEN STORAGE APPLICATIONS

N. A. NIAZ[a,b], ISHAQ AHMAD[a], S. NASIR[a], Z. WAZIR[c], R. HUSSAIN[a,d], N. R. KHALID[b], S. TAJAMMUL HUSSAIN[d]

[a]*Department of Physics, COMSATS Institute of Information Technology, Islamabad, Pakistan.*

[b]*Department of Physics, Bahauddin Zakariya University, Multan, Pakistan.*

[c]*Department of Basic Sciences, Riphah International University, Islamabad, Pakistan*

[d]*National Center for Physics, Qaid-a-Azam University Campus, Islamabad, Pakistan.*

Mg-Al system and 2mol% Ni additive nano catalyst in the particle size range of 30–45 nm were synthesized at relatively low temperature by thermal decomposition of co-precipitated $[Mg(Bipy)_2]Cl_2$, $[Al(Bipy)_2]Cl_4$ and $[Ni(Bipy)_3]Cl_2$ in an inert ambient of dry argon gas. The silvery black Mg–Al alloy and dark black Ni nanoparticles were found to be air-stable. Afterwards 2mol% Ni was added in Mg-Al system by high energy ball milling. These nano alloys were characterized by Transmission electron microscopy (TEM) Scanning electron microscopy (SEM) and X-rays diffraction (XRD) for compositional and structural analysis. Hydrogen absorption measurements were carried out using seivert'z type apparatus.

(Received November 4, 2012; Accepted February 18, 2013)

Keywords: Thermal decomposition, Mg-Al nano alloys, Hydrogen storage, P-C-T measurements, TEM

1. Introduction

Mg has attracted much interest for the future hydrogen economy due to its high theoretical gravimetric hydrogen density of 7.6 wt%, high reversible storage capacity and low cost [1-3] But suffers from several draw backs e.g. (I) Thermodynamics reveals desorption from metal hydride required high temperature [4]. (II) The kinetics of adsorption/desorption are slow [5]. (III) Magnesium is very sensitive to gaseous impurities such as oxygen, creating oxide shell, retarding kinetics and thermodynamics of hydrogen adsorption/desorption [6]. In order to improve characteristics of Mg-hydride for suitable hydrogen storage application two main fields have been explored.

First one is addition of catalyst such as 3-d transition metal or mix metal oxides. These additives change surface properties and lead to improve the kinetics [7]. The second method is the modification of thermodynamic properties by chemical alloying (substitution or addition of other elements) or through material processing (melts spinning, mechanical alloying), [8-10] binary alloys [11, 12] have been thoroughly investigated, because they have superior kinetics compared to pure Mg [13].

An alternative approach for strong non-dissociative hydrogen binding also comes from the possibility of adsorbing hydrogen molecules on light non-transition metal ions, e.g. Li^+, Na^+, Mg^{2+}, $Be^{2+}$and Al^{3+} [14]. These bare metal ions can cluster many H_2 molecules around themselves with quite strong binding energy ranging from 12–340 kJ mol^{-1}. For the alkali metals (Li^+ and Mg^{2+}) H_2 is bound through electrostatic charge quadruple and charge–induced dipole interactions[15].

*Corresponding author: niaz_ahmed@comsats.edu.pk

For Al^{3+} and Mg^{2+}, which display the highest binding energies, because of the strong orbital interactions [16].The alloying technique provides significant potential for both alloying and micro-structural modification of hydrogen storage material.

In this study pure Al-Mg alloys were prepared successfully and Ni nanoparticles were introduced as catalyst by high energy ball milling. The elemental and structural analysis of the synthesized materials are performed using XRD, SEM, EDS, TEM and at the end their efficiency for hydrogen absorption and desorption were studied by using seivert'z apparatus.

2. Experimental

Following the procedure as reported in our earlier Elsevier publication [17], these nano alloys were prepared. All the reagents and chemicals used were of analytical grade. Aluminum Chloride (Sigma Aldrich), Magnesium Chloride (Sigma Aldrich), Nickel Chloride (Sigma Aldrich), 2,2 Bipyridine (Fluka), 1-Propanol, Diethyl Ether.

2.1 Synthesis; $[Al_2 (Bipy)_2] Cl_4$

0.5 molar (7.81g/100ml) solution of bipyridine and 0.5 molar (6.67g/100ml) solution of aluminum chloride was separately prepared in 1-propanol. The bipyridine solution was transferred in dropping flask and aluminum chloride solution was added drop wise with constant stirring at a temperature of 45-50ºC. The slight pink precipitate of the aluminum bipyridyl complex appeared after almost one third of bipyridine solution was added to the $AlCl_3$ solution. Addition of aluminum chloride solution was continued till enough amount of precipitate formed in the reaction mixture. The precipitate was then filtered and washed two times with 1-propanol to remove the unreached bipyridine /aluminum chloride. At the end, precipitate was dried under IR lamp.

2.2 $[Mg (Bipy)_2]Cl_2$

1.0 molar (15.6g/100ml) solution of 2,2 bipyridine prepared in 1-propanol and 0.5 molar (4.75g/100ml) solution of magnesium chloride prepared in 1-propanol at a temperature of 40-50ºC. Bipyridyl complex of magnesium was not precipitated by the addition of bipyridine solution to the magnesium chloride, but the color of the reaction mixture changed from transparent to light orange. The solution was concentrated to two third of the original volume using rotary evaporator and then kept for crystallization. Crystallization occurred slowly, almost completed in 10 days. The crystals of the bipyridyl complex were separated through filtration, were washed two times with diethyl ether and finally vacuum dried.

2.3 $[Ni(Bipy)_3]Cl_2$

0.1 molar (1.56g/100ml) solution of 2,2 bipyridine was prepared in 1-propanol and slowly dropped using HPLC pump to 0.2 molar non-aqueous nickel chloride solution in 1-propanol, at a temperature of 50-60ºC with constant stirring. The solution was kept for crystallization and after 48 hours shiny crystals of nickel-bipyridyl were obtained. The crystals were washed with diethyl ether and finally the complex was dried under IR lamp.

2.4 Prepration of Alloys

Calculated amount of the synthesized bipyridyl complexes of aluminum and magnesium were separately dissolved in 250ml of distilled water. Both solutions were then mixed at room temperature for 30 minutes. 500ml solution of the mixed bipyridyl complexes of aluminum and magnesium was prepared. The water was very slowly evaporated at a temperature of 45-55ºC with constant stirring to get homogenous powder of both complexes. This powder was then subjected to an argon treatment in a tube furnace. The temperature of the furnace was raised to 500ºC at a heating rate of 0.5 ºC min^{-1} and the contents were kept at 500ºC for 24 hrs, then allowed to cool to

room temperature under an inert atmosphere of argon gas. This treatment yielded 63% of aluminum-magnesium (1:1).

Similar process was followed for the preparation of nickel nanoparticles. Afterward 2mol% Ni nanoparticles were added in Mg-Al system by high energy ball milling using a high-energy Spex mill.

3. Results and discussions

Fig.1(a), confirms the formation of mixed phase (β-phase) Mg_2Al_3 nano-alloys and 5-10% $Al_{12}Mg_{17}$. XRD pattern is matched with reference code (PDF#40-0903) and (PDF#01-1128). Fig. 1(b), represents XRD pattern after the hydrogenation. The Mg-Al alloys disproportionate under formation of MgH_2 and Al according to the following scheme below

$$Mg_xAl_y + xH_2 \rightarrow xM_gH_x + yAl$$

The reason for disproportion of Mg-Al alloys during hydrogenation is due to relatively high thermodynamic stability of MgH_2 compared to alloy combined with a relatively low stability of Mg-Al-H compound [18-19].

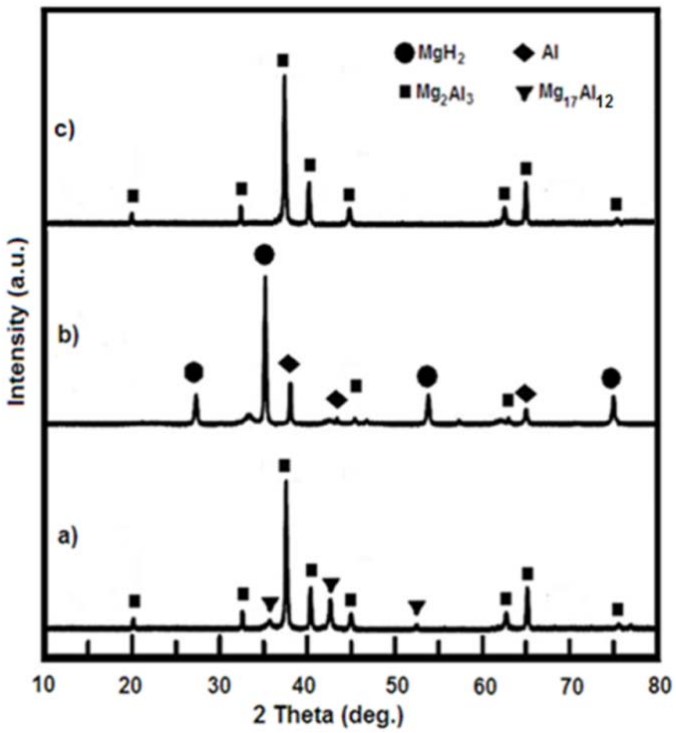

Fig. 1(a) XRD pattern Mg-Al nano alloys before hydrogenation; (b) after hydrogenation; (c) after dehydrogenation.

During dehydrogenation Mg and Al react and an Mg-Al alloy is formed [20] as illustrated in Fig. 1(c). In hydrogenated state only MgH_2, Al and two very small peak of Mg_2Al_3 are also shown in Fig.1 b which might be due to presence of 5-10% $Mg_{17}Al_{12}$ phase present in Fig. 1(a).

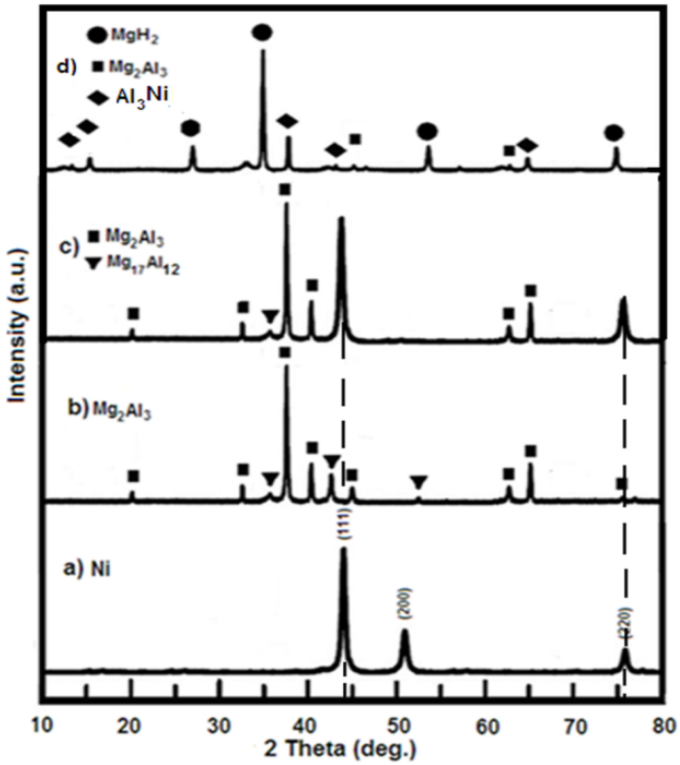

Fig. 2 XRD pattern (a) Pure Ni; (b) Al-Mg nano alloys; (c) After high energy milling Mg-Al nano alloys with 2mol% Ni; (d) after hydrogenation.

After the dehydrogenation diffraction peaks from MgH_2 and Al are absent and only those corresponding to Mg-Al alloys (β-phase) are present as conformed in Fig. 2(c).

The XRD data shows that single phase alloys Mg_2Al_3. Fig. 2, shows XRD pattern of pure Ni nanoparticles and Mg-Al alloys, présent almost single phase without impurity. After 20-30 min ball milling with Ni contents, the diffraction peaks of Mg-Al alloys were broadened and their intensities decreased, which indicates that grain size refinement and accumulation of strains occured in the alloys [22].

Fig. 2(d) clarify the hydride formation by addition of Ni in Mg-Al alloys. XRD pattern also shows that Al_3Ni compound formed, while Mg_2Al_3 phase disappeared. Very small peaks of Mg_2Al_3 are also observed in the compound after hydrogenation, that might be due to $Mg_{17}Al_{12}$ phase. It has also been observed that addition of Ni to Mg-Al alloys, tends to formation of stable Al_3Ni phase and Mg_2Al_3 phase appears to be limited by retaining amount of Al insufficient in reacting with Mg after desorption, resulting in the formation of the surplus Mg.

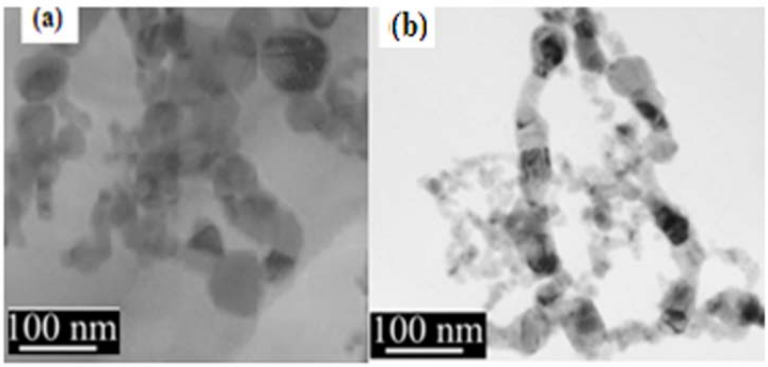

Fig. 3 TEM image of (a) Mg-Al nano alloys; (b) Ni nanoparticles

Fig. 3 represents transmission electron micrograph of Mg-Al nano alloys and Ni nanoparticles. Particle size of Mg-Al nano alloys is larger as compare to the Ni nano particles. It reveals that the compounds are nano particles.

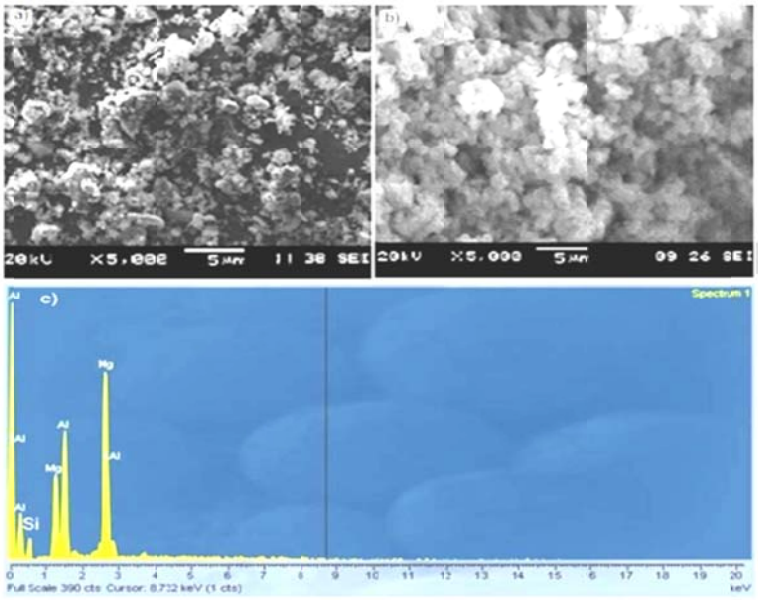

Fig. 4 SEM image of Mg-Al nano alloys; (a) before hydrogenation; (b) after hydrogenation; (c) EDX spectrum of Mg-Al alloys.

Scanning electron microscopy (SEM) represented in Fig. 4, of Mg-Al alloys show morphology and elemental analysis before and after hydrogenation. Fig. 4(a), before hydrogenation the compound particles are homogenously dispersed and elongated in irregular shape. These show high volumetric density of metal-metal interface [23]. After hydrogenation some white patches were which confirm the formation of Al metal as described in XRD results Fig. 1 (b). EDX results shown in Fig.4, confirms the elemental conformation in the compound.

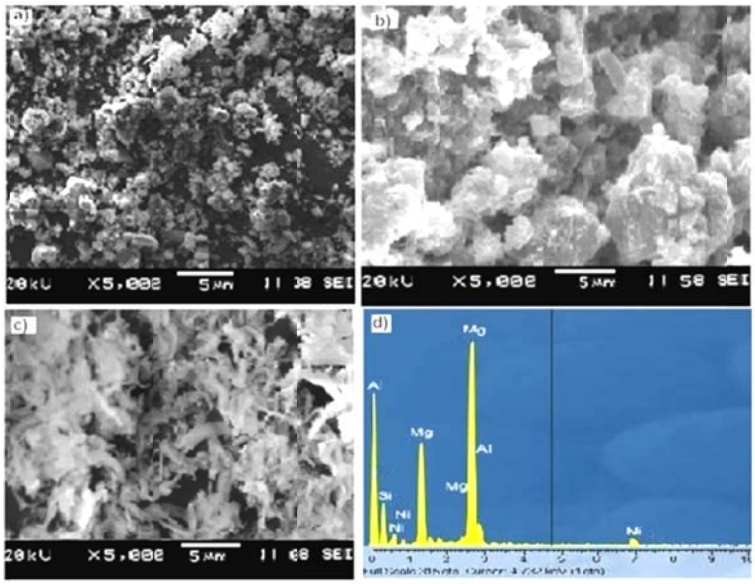

Fig. 5 SEM micrograph (a) Mg-Al alloys; (b) Ni nanoparticles; (c) (Mg-Al alloys +2mol% Ni) after high energy ball milling; (d) EDX pattern of after ball milling

SEM image shown in Fig. 5, demonstrate morphology of Mg-Al alloys, Ni nanoparticles and after high energy ball milling 2mol% Ni with Mg-Al alloys. Fig. 5 c, indicates that particles are in irregular shape and irregular grain boundaries confirming that particles have volumetric density and trimetallic interconnected domains after ball milling. It is also clear from SEM image that grains of Mg-Al alloys are surrounded by Ni inter-grain regions which improved the hydrogen absorption. Fig.5 d EDX pattern shows that no impurity exists in the compound.

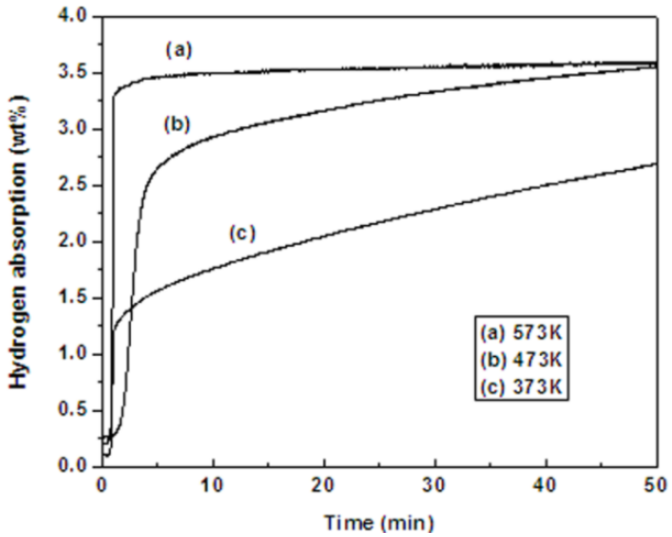

Fig.6 Hydrogen absorption results of Mg-Al nano alloys at different temperatures; (a) 373K; (b) 473K; (c) 573K.

Hydrogen storage ability of Mg-Al alloys at different temperature has been identified in Fig. 6. At 573K, a fabulous hydrogen absorption behavior was observed which may be due to defective surface having large number of grain boundaries as observed in SEM micrograph Fig. 4(a). From Mg-based alloys, the hydrogenation appears to be limited by diffusion process, with Al act as a heat-transfer medium [23-24], causes the fast absorption rate of the compound. Low temperature i.e. 373K absorption rate is very sluggish.

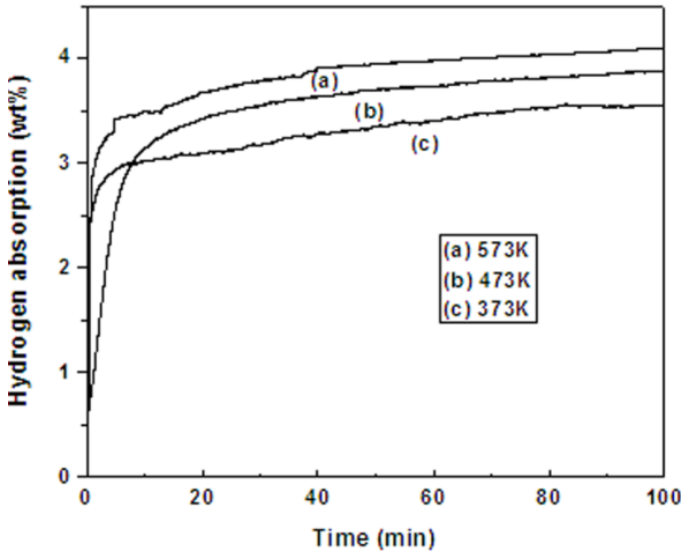

Fig.7 H_2 absorption results of Mg-Al nano alloys catalyzed by 2mol% Ni nanoparticles at different temperature.

Hydrogen absorption rate of Mg-Al alloys catalyzed by 2mol% Ni nanoparticles has been presented in Fig.7. Very sharp increase in hydrogen absorption has been observed as compared to pure Mg-Al alloys as shown in Fig. 6 at 373 K. The SEM micrograph shows after high energy ball

milling, the surface of the compound becomes defective and particle size reduced, causes the improvement in hydrogen absorption rate.

The hydriding properties of the alloys improved due to the large volume fraction of the grain boundaries region as comprehensible from SEM image. The fine grain boundaries also favor hydrogen migration and residence resulting in a high storage capacity. This difference contributes significantly towards the hydrogen absorption and desorption properties between two materials. Both Al and Ni dissolution into Mg lattice should decrease the lattice parameter and hence decrease the hydride dissociation temperature [25-26].

Mg-Al matrix provides a great number of diffusion channels and interstitial sites for hydrogen migration and Ni behaves as cluster network surrounding the Mg-Al matrix [27-28]. This plays a catalytic role during hydrogen absorption/desorption mechanism. The hydrogen storage capacity at room temperature increases if the Ni phase is distributed homogenously on the Mg matrix [29]. Consequently we can suggest that addition of Ni, electronically modify the surface geometry of the system with lower activation energy and bimetallic active sites. This may be due to change in the hybridization chemistry of Mg-Al alloys by the addition of Ni, which specifies the specific phase of the material.

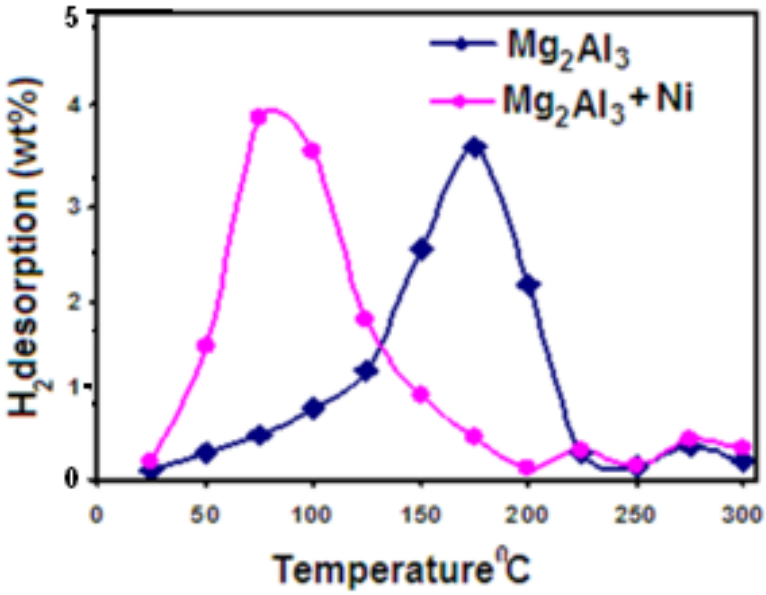

Fig. 8 H_2 desorption results by temperature program desorption (TPD) Mg-Al nano-alloys and 2mol%Ni catalyzed Mg-Al nano-alloys.

Desorption occurs when molecules detached from the surface by increasing temperature. When molecules come in contact with a surface, they are adsorbed, minimizing their energy by forming a chemical bond with the surface. The binding energy varies with the combination of the adsorbate and the surface. If the surface is heated, the energy transferred to the adsorbed species causes it's desorption. The temperature at which this phenomenon occurred reflects the characteristics of alloys formation. Species previously adsorbed can be desorbed into a stream of pure carrier gas to generate a characteristics fingerprint. The different configuration of valence electron of Al than Ni may also contribute for high desorption properties of Ni doped Mg-Al alloys.

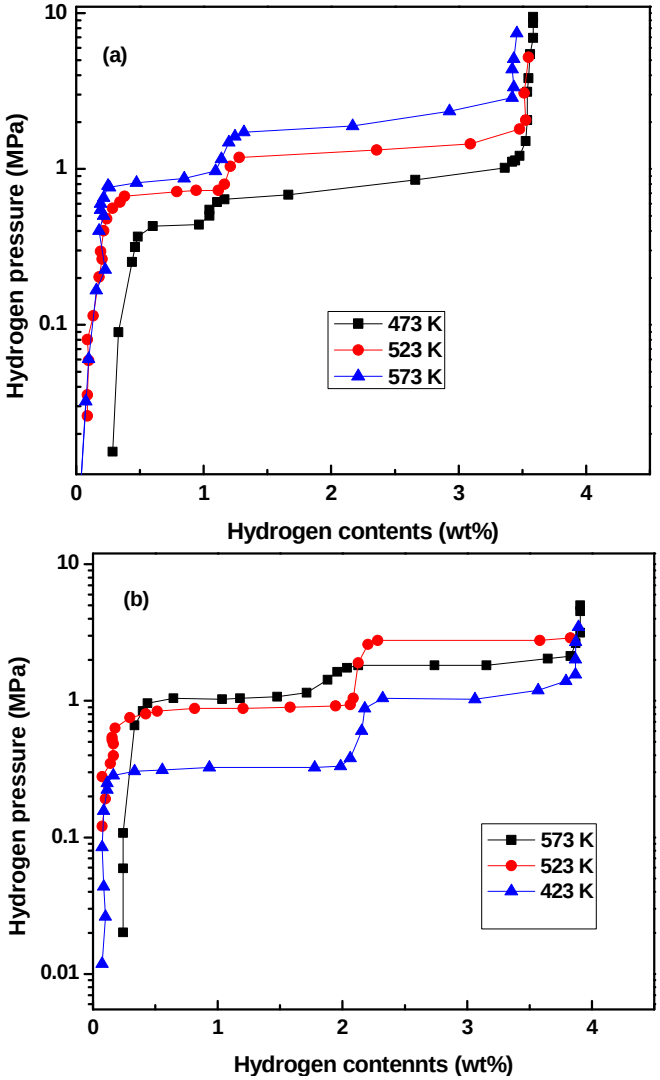

Fig. 9 PCI curves of (a) Pure Mg-Al alloys (b) 2mol%Ni catalyzed Mg-Al nano-alloys.

In order further to investigate the effect of Ni on the hydrogen absorption properties of Mg-Al alloys, equilibrium pressure hydrogen absorption were performed using PCI measurements at different temperatures. From Fig. 9(a), pure Mg-Al alloys correspond to a two step transformation reaction. Single plateau associated with decomposition of Mg_2A_3 as into MgH_2 and Al shown in Fig.1, XRD pattern.

Fig.9(b), represents the hydrogen absorption behavior of 2mol%Ni catalyzed Mg-Al alloy. At 473 K only one plateau was observed, whereas at higher temperature 573 K very clear high and low plateau was observed, which may be because of $Mg_{17}Al_{12}$ contents as observed in Fig. 2, which is decomposed into Mg_2Al_3 and further decomposition of Mg_2Al_3 into MgH_2 and Al [30]. About 4wt% hydrogen absorption was estimated in PCI pattern.

4. Conclusion

Pure Mg-Al alloys and Ni nanoparticles prepared by thermal decomposition on bipyridyl complex of metals, which is alternate route for the preparation pure alloys. By the addition of 2mol%Ni by high energy ball milling, grain refinement take place which cause the defects on the surface that might be useful for hydrogen absorption/desorption properties. Hydrogen absorption rate of 2mol% Ni catalyzed Mg-Al alloys is extremely better than pure Mg-Al alloys at low temperature. The substitution of transition metal (Ni) in Mg-Al leads to significant modification of

shape and width of valence band of nano alloy which play a critical role for hydrogen absorption/desorption properties.

Acknowledgement

Higher Education Commission of Pakistan Indigenous-5000 Fellowship and HEC "IRSIP" Program

References

[1] J. L. Bobet, E. Akiba, B. Darriet, I. J. Hydrogen Ener., **25**, 987, (2000).
[2] X. Yao, G. Lu, Chinese Scie. Bull., **53**, 2421, (2008).
[3] Z.X. Guo, C. Shang, , K.F.. Aguey-Zinsou, J. Europ. Cera. Soc., **28**, 1467, (2008).
[4] B. Sakintuna, F. Lamari-Darkrim, M. Hirscher, I. J. Hydrogen Ener., **32**, 1121, (2007).
[5] M. Jurczyk, I. Okonska, M. Nowak, M. Jarzebski, J. Optoelectron. Adva. Mate. **10**, 907, (2008).
[6] H. Reule, M. Hirscher, A. Weibhart and H. Kronmuller, J. Alloy.& Comp., **305**, 246, (2000).
[7] T. I. Nobuko Hanada, F. Hironobu J. Phys. Chem. B, **109**, 7188, (2005).
[8] G. Friedlmeier, M. Arakawa, T. Hiraia, J. Alloy.& Comp., **292**, 107, (1999).
[9] S. Kalinichenka, L. Röntzsch, C. Baehtz, B. Kieback, I. J. Hydro. Ener., **35**, 12829, (2010).
[10] P.Selvam, K.Yvon, Int. J. Hydr. Ener., **16**, 615, (1991).
[11] Y. Zhang, Y.Tsushio, H Enoki, E.Akiba, J. Alloy.& Comp., **393**, 147, (2005).
[12] L. Baum, M. Meyer, Mendoza-Zélis, Physica B: Condensed Matter, **389**, 189, (2007).
[13] G. Liang, R. Schulz, J. of Alloy. & Comp., **356**, 612, (2003).
[14] E. David, J. Mater. Proce. Tech., **162**, 169, (2005).
[15] Y. Nakamori, S. Orimo, T. Ekino, H. Fujii, J. Alloy.& Comp., **404**, 396, (2005).
[16] T. Mizoguchi, I. Tanaka, Microscopy and Microanalysis, **11**, 1444, (2005).
[17] N. A.Niaz, Waheed S. Khan, I. Ahamd, S. Tajammul Hussain, J. Mate. Scie.& Tech. **28**, 401, (2012)
[18] J. S. C. Jang, J. Y. Ciou, T. H. Hung, J. C. Huang, X. H. Du, Adv. Eng. Mater. **10**, 1048, (2008).
[19] A. Andreasen, I. J. Hydrogen Ener., **33**, 7489, (2008).
[20] X.Y. Liu, J.B. Adams, Sur. Sci., **373**, 357, (1997).
[21] M. Sterlin, H. Leo, I. J. Hydrogen Ener. **32**, 4933, (2007).
[22] H. Gu, Y. Zhu, L. Li, I. J. Hydro. Ener., **33**, 2970, (2008).
[23] T.Spassov, P.Solsona, S.Bliznakov, S. Suriñach, MD Baró, J. Alloy.& Comp., **356**, 639, (2003).
[24] A. S. Palma, J.L. Iturbe-García, B.E. López-Muñoz, I. J. Hydrogen Ener., **35**, 12120, (2010).
[25] C. Wu, P. T. Williams, Applied Catalysis B: Environmental, **96**, 198, (2010).
[26] X. Xiao, L Chen, Z Hang, X Wang, S Li, C Chen, Elect. Commun., **11**, 515, (2009).
[27] E. Grigorova, M. Khristov, M. Khrussanova, J. Alloy.& Comp., **414**, 298, (2006).
[28] S. T. Hussain, N. A. Niaz, I. Ahmed, R. Hussain, I. Rev.Chem. Eng., **1**, 238, (2009).
[29] M. Martin, C. Gommel, C. Borkhart, E, Fromm, J. Alloy. & Comp., **238**, 193, (1996).
[30] S.L. Lee, C.W. Hsu, F.K. Hsu, C.Y. Chou, C.K. Lin, Mater. Chem.& Phys., **126**, 319 (2011).